European Polymer Journal 46 (2010) 1184–1193

Contents lists available at ScienceDirect

European Polymer Journal

journal homepage: www.elsevier.com/locate/europolj

Macromolecular Nanotechnology

Crystal growth of $CaCO_3$ induced by monomethylitaconate grafted polymethylsiloxane

Andrónico Neira-Carrillo [a,b,*], Patricio Vásquez-Quitral [a], Mehrdad Yazdani-Pedram [b,c], José L. Arias [a,b]

[a] Faculty of Veterinary and Animal Sciences, Santa Rosa 11735, P.O. Box 2-15, University of Chile, Santiago, Chile
[b] Center for Advanced Interdisciplinary Research in Materials (CIMAT), Av. Beaucheff 850, Box 2777, Santiago, Chile
[c] Faculty of Chemistry Science and Pharmaceutics, Olivos 1007, P.O. Box 233, University of Chile, Santiago, Chile

ARTICLE INFO

Article history:
Received 31 August 2009
Received in revised form 17 February 2010
Accepted 9 March 2010
Available online 11 March 2010

Keywords:
Gas diffusion method
Hydrosilylation reaction
Monomethylitaconate
Calcium carbonate
Vaterite
Calcite

ABSTRACT

We report the preparation of a new monomethylitaconate grafted polymethylsiloxane (CO_2H-PMS) copolymer and its effect as template for crystal growth of $CaCO_3$. The *in vitro* crystallization of $CaCO_3$ was carried out using the gas diffusion method at different pH values at room temperature for 24 h. The CO_2H-PMS was prepared using polydimethylsiloxane-*co*-methylhydrogensiloxane (PDMS-*co*-PHMS), obtained through cationic ring opening polymerization, from cyclic monomers and monomethyltaconate (MMI) via hydrosilylation reactions with platinum complex as catalyst. FTIR results are in an agreement with the proposed template structure and confirmed that the hydrosilylation was complete. Experimental results from pH values and SEM analysis showed that the carboxylate groups of CO_2H-PMS alter the nucleation, growth and morphology of $CaCO_3$ crystals. SEM revealed single-truncated (ca. 5 μm) modified at pH 7–9, aggregated-modified (ca. 20 μm) at pH 10–11, and donut-shaped crystals at pH 12. These morphologies reflect the electrostatic interaction of carboxylic moieties with Ca^{2+} modulated by CO_2H-PMS adsorbed onto the $CaCO_3$ particles. EDS confirmed the presence of Si atoms on the crystals surface. XRD analysis showed the existence of only two polymorphs: calcite and vaterite revealing a selective control of $CaCO_3$ polymorphisms. In summary, the use of grafted polymethylsiloxane template offer a good alternative for polymer controlled crystallization and a convenient approach for understanding the biomineralization process useful for the design of novel materials.

1. Introduction

The biological crystallization (biomineralization) is the process by which living organisms produce biological composites (mollusk and egg shells, crustacean carapaces, bones, teeth) and exert accurate control over the minerals they deposit, creating materials with uniform particle size, novel morphology, myriad shapes and sizes that are often of high strength and remarkable properties [1,2]. Molecular processes involved in biomineralization and materials that control such crystal nucleation and growth are of great interest to materials scientists who seek to manufacture composite materials with analogous crystalline forms to those produced by nature. Calcium carbonate ($CaCO_3$) is one of the most studied systems, which can facilitate the understanding of biological control of biomineralization [3,4]. $CaCO_3$ crystals have three polymorphs: calcite (trigonal), aragonite (orthorhombic), and vaterite (hexagonal). $CaCO_3$ biominerals usually consist of single-crystals intimately associated with macromolecular organic matrices. Calcite is one of the most common biomineral phase. For instance, some calcite biominerals are produced as skeletal elements that behave as single-crystals, such as sponge

* Corresponding author. Address: Faculty of Veterinary and Animal Sciences, Santa Rosa 11735, P.O. Box 2-15, University of Chile, Santiago, Chile. Tel.: +56 2 9785642; fax: +56 2 9785526.
E-mail address: aneira@uchile.cl (A. Neira-Carrillo).

0014-3057/$ - see front matter © 2010 Elsevier Ltd. All rights reserved.
doi:10.1016/j.eurpolymj.2010.03.008

spicules [5,6] and sea urchins spicules [7]. Other biominerals are partly composed of single-crystalline calcite subunits, such as the prismatic layers of many mollusk shells [8]. Thus, mollusk shells are mainly built of two polymorphs of $CaCO_3$: calcite and aragonite. Precipitation of such biominerals take place in confined microenvironments under chemical control of the adjacent cells [9]. Therefore, there are several approaches for exploring the promoting effect of templates on *in vitro* inorganic crystallization. In fact, many approaches have been used to synthesize a specific form of $CaCO_3$ by using different materials as templates such as films, spheres, sponge, ligand–receptor complexes, block copolymers, synthetic polypeptides and grafted polymers, etc. The crystallization mechanism can be altered by specific interactions with chemical moieties like: $-CO_2H$, $-PO_3H$, $-SO_3H$ [10–14]. Water-soluble block copolymers with a polyelectrolyte block turned out to be extraordinarily effective crystal growth modifiers [15–17]. Different factors can affect the crystal growth and the crystal morphology. These include mineralization solution pH, temperature, saturation, crystallization method, reactants concentration and additives, e.g., polymers [18]. The resulting morphology of synthetic crystals is an expression of different growth rates in the various crystallographic directions. From a thermodynamic point of view, the obtained crystal morphology minimizes the free enthalpy of the crystal which is the sum of the products of surface energy and area of all exposed faces (Wulff's rule) [19]. This has the consequence that low energy surfaces become exposed and high energy surfaces vanish. Crystal surface energies can be lowered by the adsorption of additives present in solution and the crystal morphology alters correspondingly [20]. According to Wulff's rule, planes on which the additives are adsorbed become generally expressed as crystals faces [21]. The appropriate use of polymers in the processing of inorganic substances can result in new hybrid materials, with specific structure, advanced properties and functions [22]. Abundant studies on $CaCO_3$ crystallization addressing biological control over mineralization have been done applying organic substrates as additives. Polyanionic macromolecules have been reported to mediate mineralization by forming aggregates with mineral ions [23]. Functionalized macromolecules are also involved in the temporary stabilization of amorphous precursor phases, which occur as a transient phase in formation of sea urchin calcite skeletons [24]. Organic polyanions have been found within the biominerals as intercrystalline matrices [25–27], suggesting that precipitation mediating molecules may partly become incorporated during crystallization. Few reports have appeared on controlling the $CaCO_3$ nucleation and crystal growth, where biomineralization is mediated by employing inorganic templates and poly(organosiloxane)s [28]. Polysiloxanes (PMS) usually referred to as silicones, find numerous applications in different fields of chemistry and engineering. PMS also represent the most widely used silicon-containing polymeric systems in different industrial and medical applications [29,30]. Polydimethylsiloxane (PDMS) and polyhydrogenmethylsiloxane (PHMS) are well known for their versatile properties such as flexibility, permeability to gases, low glass transition temperature and low surface energy. They are physiologically inert, biocompatible and exhibit convenient cost-benefit ratio. All these applications rely on the unique physical and chemical properties of silicones in the bulk form and at interfaces. Widely applied and recently explored hydrosilylation reaction of polymers have attracted great interest due to the practical outcome and recent development in silicon-based organic polymers [31,32]. The main synthetic route leading to the modification polysiloxanes is the hydrosilylation reaction of unsaturated compounds such as allyl derivatives with polysiloxanes containing Si–H labile group by using platinum catalysts [33]. Speier's catalyst is the most commonly used catalyst for these reactions [34]. From the above mentioned, the PMS polymers become very attractive as new templates for *in vitro* crystallization assays [35,36]. Although abundant articles on the production of modified PMS for both medical and non-medical applications have appeared [37–41], the available information concerning the effect of PMS on biomineralization of $CaCO_3$ is scarce. PMS can be chemically modified with different chemical group's counterparts as those existing on the surface of organic molecules, emulating the guide role of these during the *in vivo* crystallization. Herein, we report the synthesis of a new PMS grafted with monomethylitaconate produced by hydrosilylation reaction through the dicyclopentadienyl platinum II chloride (Cp_2PtCl_2) obtained from the Speier's catalyst and its effect as an inorganic–organic template on crystal growth of $CaCO_3$ *in vitro* using a gas diffusion method [42]. The Cp_2PtCl_2 catalyst is not commercially available [43]. In the present article we have demonstrated that the spatial arrangement of carboxylic groups attached to PMS (CO_2H-PMS) can alter the nucleation and morphology of $CaCO_3$ and our results demonstrate that CO_2H-PMS can effectively stabilize the less thermodynamically stable polymorph, i.e., vaterite as a function of pH at room temperature. Additionally, our report is motivated by the paucity published works with PMS in biomimetic mineralization field. With this in mind, carboxyl group of modified CO_2H-PMS was conjugated to primary amine group of chitosan (CHI) using 1-ethyl-3-(3-dimethylaminopropyl) carbodiimide (EDC). Thus, different CHIs grafted polysiloxanes (CO_2H-PMS-*g*-CHI) ratio were prepared and then coupled with gold nanoparticles (AuNP ~12 nm) and its influence on the $CaCO_3$ crystallization evaluated.

2. Experimental

2.1. Materials

Calcium chloride, ethanol, sodium hydroxide (Analytical grade) and tris(hydroxymethyl) aminomethane (TRIS), petroleum benzene (Aldrich-98% boiling range 40–60 °C) and toluene (99.9%) were obtained from Merck; ammonium hydrogen carbonate (NH_4HCO_3) was from J.T. Baker and methylene chloride (CH_2Cl_2 – ⩾99.5%) from Sigma-Aldrich. These reagents were of the highest available grade. The distilled water was obtained from capsule filter 0.2 μm flow (U.S. Filter). Toluene and methylene chloride were dried and distilled under argon. Both were purified by refluxing over lithium aluminum hydride (Aldrich-95% pellets particle size 10×6 mm) for 72 h and Na, respectively. The

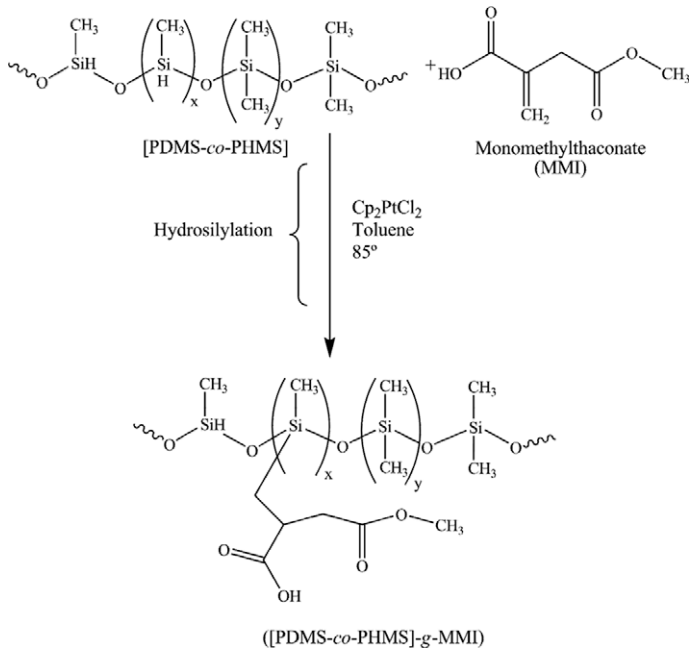

Fig. 1. Synthesis of CO_2H-PMS.

dicyclopentadienyl platinum (II) chloride (Cp_2PtCl_2) catalyst used for the hydrosilylation reaction was synthesized from hydrated hexachloroplatinic acid (IV) and diclyclopentadiene [43]. The monomethylitaconate (MMI) was synthesized by direct esterification of itaconic acid (Aldrich) with methanol and its purity was checked by ^1H NMR spectroscopy as described in a previous work [44]. The PDMS-*co*-PHMS (M_W of 16,349 g/mol and polydispersity of $D = 2$) was synthesized through cationic ring opening polymerization from octamethylcyclosiloxane (D_4) and 1,3,5,7-tetramethylcyclotetrasiloxane (D_4^H). The PDMS-*co*-PHMS ($\chi^0_{D_4} = 0.5$) was used for hydrosilylation reaction with purified MMI [43]. A purified CHI sample was used for the preparation of chitosan grafted polysiloxanes ratio. The purification of commercial CHI ($M_w = 70$ KDa, >75% deacetylation) obtained from Fluka were done as previously reported [45]. The 1-ethyl-3-(3-dimethylaminopropyl) carbodiimide (EDC) was used as received from Sigma-Aldrich without purification.

2.2. Hydrosilylation reaction

The hydrosilylation reaction of PDMS-*co*-PHMS with MMI as unsaturated compound was carried out using Cp_2PtCl_2 as catalyst [46,47]. Briefly, MMI (20 mol.% excess versus the Si–H of copolymer) was dissolved in 100 ml of sodium-dried, freshly distilled toluene together with the stoichiometric amount of PDMS-*co*-PHMS. The reaction mixture was heated to 85 °C under argon and 100 μl of Cp_2PtCl_2 as a solution in CH_2Cl_2 was then injected. The mole ratio of Pt/SiH catalyst was 1.5×10^{-4}. Then, the mixture was refluxed under argon with agitation until the FTIR showed that the hydrosilylation reaction was complete (ca. 24 h). After removing the excess of solvent and the unreacted materials with a Heidolph rotary evaporator (Laborota 4001 efficient-HB digital) at 90 rpm under vacuum at 70 °C for 1 h. The product was precipitated with petroleum benzene. The supernatant was separated and the resultant CO_2H-PMS was dried at 90 rpm under vacuum at 50 °C for 2 h. The yield from the hydrosilylation was 95%. The synthetic route for the preparation of CO_2H-PMS after the hydrosilylation reactions is shown in Fig. 1.

2.3. In vitro crystallization of calcium carbonate

Crystallization experiments were carried out in the presence of CO_2H-PMS as additive and compared with PDMS-*co*-PHMS as negative control using the gas diffusion method (Fig. 2). The gas diffusion method was performed as we described in previous works [47–52]. Briefly, a chamber consisting of an 85-mm polystyrene Petri dish having a central

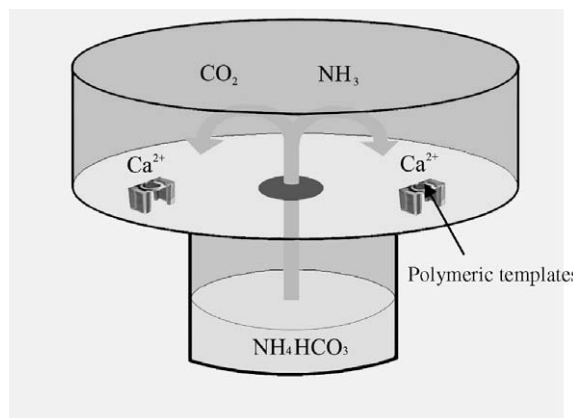

Fig. 2. Experimental setup for the gas diffusion crystallization.

hole in its bottom is glued to a cylindrical vessel. Inside the chamber, polystyrene microbridges were filled with 35 μl of 200 mM $CaCl_2$ solution in 200 mM TRIS buffer. The cylindrical vessel contained 3 mL of 25 mM NH_4HCO_3 solution. All experiments were carried out inside the Petri dish using both polymer templates at 1.0 mg/mL concentration at 20 °C for 24 h. A microbridge was filled with a 35 μl of $CaCl_2$ solution without additive as control. For these experiments a stock solution of 1.6 mg of CO_2H-PMS in deionized water at different pH (from 7 to 12) was prepared as mother solution in an Eppendorf tube. On the other hand, the same crystallization procedure was used when CHI grafted polysiloxanes (CO_2H-PMS-*g*-CHI) and its coupled product with AuNP were carried out. A set of experiments were done using different pH, from 7 to 12, at 20 °C for 24 h. $CaCO_3$ crystals resulted from the diffusion of carbon dioxide (CO_2) into the buffered $CaCl_2$ solution. The microbridges with the $CaCO_3$ crystals were carefully rinsed with deionized water and dehydrated by using ethanol solution of growing concentrations (50%, 80%, 90% and 100%), dried at room temperature and observed by SEM.

The crystal growth of $CaCO_3$ can be simplified by the following equations:

$$(NH_4)HCO_{3(ac)} = CO_{2(g)} + 2NH_{3(g)} + H_2O_{(ac)} \quad (1)$$

$$CO_{2(g)} + CaCl_{2(ac)} + 2NH_{3(g)} + H_2O_{(ac)} = CaCO_{3(s)} + 2NH_4Cl_{(g)} \quad (2)$$

2.4. Measurements

Fourier transform infrared spectroscopy (FTIR) of PDMS-*co*-PHMS, CO_2H-PMS and CO_2H-PMS-*g*-CHI templates were obtained on a Bruker Vector 22 and Varian 1000 Acimitar Series instruments. The samples were prepared as potassium bromide pellets. The molecular weight (M_W) determination of PDMS-*co*-PHMS copolymer was carried out by using PSS-Win GPC-PSS Gel Permeation Chromatography (GPC). The $CaCO_3$ crystals formed after *in vitro* crystallization were dried, fixed to a metal support and then coated with gold using an automated sputter coater (EMS-550). Crystals of $CaCO_3$ formed in the presence of PDMS-*co*-PHMS as negative control and with CO_2H-PMS template were observed in a Tesla BS 343 A microscope at 15 keV. SEM-EDS analyses of $CaCO_3$ crystals were performed in a SEM LEO 1420VP equipped with a dispositive for microanalysis of elements in surface and linear profile. TEM images of CHI grafted PMS coupled with AuNP were performed on an EM 912 Ω (Zeiss). XRD analyses of the resultant crystals were made in Siemens D-5000X X-ray diffractometer with CuK_α radiation (graphite monochromator) and an ENRAF Nonius FR 590 diffractometer. The geometric scanning Bragg-Brentano (θ–θ) and the angle range from 5° to 70° (2θ) were performed. The Diffrac Plus software was used as data control.

3. Results and discussions

The term hydrosilylation refers to an addition reaction of Si–H bonds to double bonds such as C=C and represents one of the most fundamental method for the laboratory and industrial synthesis of organosilicon compounds and organic silyl derivatives [41]. The hydrosilylation reaction of the starting PDMS-*co*-PHMS was monitored by FTIR technique following the decrease of the Si–H bond. Fig. 3 represents the FTIR spectra of PDMS-*co*-PHMS, MMI and CO_2H-PMS. Fig. 3A shows a classic FTIR spectrum of an organosilicon in which the most typical absorption peaks are at 2967, 2160, 1260, 1105 and 801 cm^{-1} corresponding to C–H, Si–H, Si–CH_3 and Si–O–Si, respectively [53,54]. For the MMI structure, the Fig. 3B showed the absorption bands due C–H and C=O at 2958 and 1729 cm^{-1}, respectively. In the Fig. 3C, the absorption band of Si–H from the PDMS-*co*-PHMS (Fig. 3A, arrow) disappeared completely demonstrating the effectiveness of the hydrosilylation reaction. The absorption bands at 2961 cm^{-1} are assignable to the incorporation of carbon/hydrogen bonds on the main chain of the CO_2H-PMS template. The presence of the principal groups such as carboxylic, carbonyl and silicon–oxygen ester bonds of the grafted CO_2H-PMS corresponding to the bonds O–H, C=O and Si–O–Si can be recognized at 3502, 1741 and 1099 cm^{-1}, respectively. The absorption band observed at 1741 cm^{-1} (Fig. 3C, arrow) is due to the carboxyl group of the ester linkage of MMI and confirms its incorporation in the new CO_2H-PMS template. Similar position of this absorption band of MMI has been observed with polyethylene chains [55]. The absorption bands at 126 and 808 cm^{-1} confirm also the presence of Si–CH_3 and Si–O–Si bonds.

In order to evaluate the effect of carboxylate moieties of CO_2H-PMS as an inorganic additive on *in vitro* $CaCO_3$ mineralization, a set of $CaCO_3$ crystallization experiments was performed and the morphology of the resultant $CaCO_3$ crystals were observed. The $CaCO_3$ crystallization was carried out with a gas diffusion method by varying the pH mineralization solution at 20 °C for 24 h. Fig. 4A shows the morphology of rhombohedral calcite crystals obtained without additive as blank, and in the Fig. 4B calcite crystals with similar $CaCO_3$ morphology obtained with PDMS-*co*-PMHS without carboxylic groups as negative control. However, in the Fig. 4C–H are shown different morphologies of $CaCO_3$ crystals obtained in the presence of CO_2H-PMS as template. We observed that aggregates of $CaCO_3$ crystals lost their well developed edges and show elongation on the atomic steps of the {104} face. Similar morphology of calcite crystals with stairstep dendritic structures obtained by using synthetic peptides and a synthetic organic polymer such as polyvinyl alcohol has been reported [56,57]. It is known that polysiloxanes have a much higher permeability to gases than other synthetic polymers which can be useful in the gas diffusion method. This can be explained by the torsion and bending flexibility of CO_2H-PMS as an organosiloxane compound, which elicits a characteristic nucleation and growth of $CaCO_3$ crystals. Similar results has been reported with sulfonic acid-based hydrogels in a polyacrylamide network [58] using double-diffusion crystallization and with polycarboxylate polymers as an additive [59,60]. Taking this into account we suspect that the CO_2H-PMS is adsorbed on the $CaCO_3$ surface and the presence of the carboxylate moieties bonded to the polymer backbone produce a local Ca^{2+} ions accumulation, which is more pronounced at higher pH. In fact, at pH 12 (Fig. 4H)

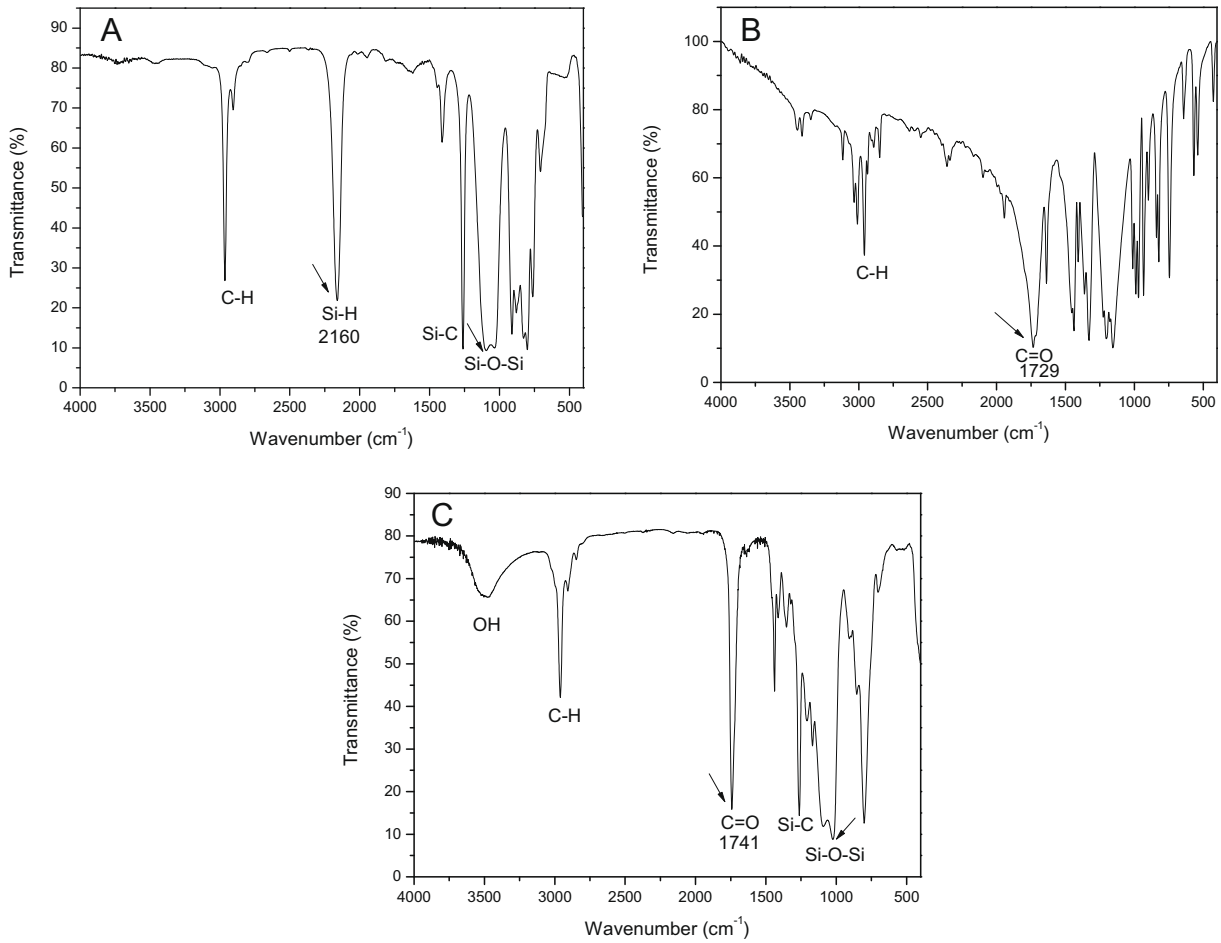

Fig. 3. FTIR spectra of (A) PDMS-*co*-PHMS, (B) MMI and (C) CO_2H-PMS.

the less thermodynamic stable polymorph, vaterite (with donut-like crystals) was obtained. The stereochemical interaction of this new template with the $CaCO_3$ surface and subsequent growth of crystals by blocking the {1 0 4} face can be visualized in the model presented in Fig. 8. Although most polyelectrolytes used to effectively control crystallization of $CaCO_3$ are block copolymers, recently, commercial random sequences of styrenesulfonate and maleic acid monomers (PSS-*co*-MA) have been reported by Cölfen et al. [61]. The PSS-*co*-MA showed effective influence on the nucleation, growth, orientation and morphology of $CaCO_3$. The influence of the polymeric template on the nucleation of $CaCO_3$ can be explained by a nanoparticles-based crystallization pathway resulting in truncated crystals.

Additionally, EDS analysis was carried out in order to investigate the presence of Si atoms on the $CaCO_3$ crystals. EDS measurements of $CaCO_3$ crystals obtained at different pH values (Fig. 5A, for pH 9) and (Fig. 5B, for pH 12) detected different amounts of Si adsorbed on the elongated calcite crystals, which demonstrates the strong inhibitory properties of CO_2H-PMS. A small amount of Si from the new template on the surface, in the range of 0.03 (at pH 9) and 0.07 (at pH 12) was enough to modify $CaCO_3$ crystals morphology. It is well known, since a long time [62], that biomineralizations such as mollusk shells, crustacean carapaces, eggshells, contain a small amount of organic molecules (0.1–4 wt.%) responsible, notably, for the polymorph and the morphology of the biomineral considered. Although, EDS is a surface technique, in the present paper the EDS was used as qualitative but spatially resolved analysis to detect the adsorption sites of the CO_2H-PMS. For this reason, EDS measurements were carried out avoiding the main error sources particularly the EDS signals from the substrate components, carbon thin films were used to protect the reference sample against environmental corrosion and to place the crystalline particles in inert ambient air reducing the environmental oxidation of the thin film surface. The contribution of these error sources decreases as the film thickness of sample increases and it is strongly dependent on the energy of the incident electron beam. A detailed description for reducing the influence of error sources, by using stoichiometric ratio of, e.g., FeS_2 thin films, reported by Ares et al. [63]. The elemental ratios of crystal particles obtained with CO_2H-PMS were determined by comparison with values obtained from pure $CaCO_3$ crystals of known chemical composition, which served as a calibration set. The C, O, Ca and Au elements were analyzed and the results were normalized by a

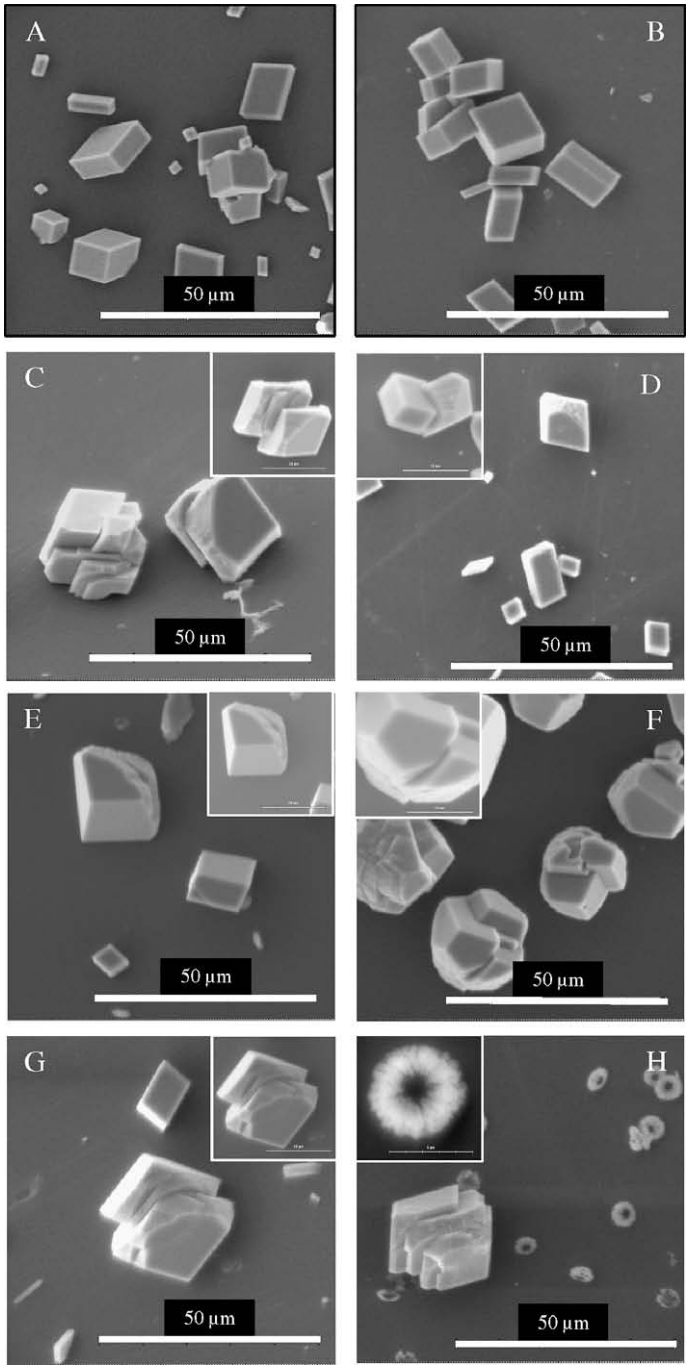

Fig. 4. SEM of $CaCO_3$ crystals of control (A), with PDMS-*co*-PHMS (B) and with CO_2H-PMS at different pH value from 7 to 12: pH 7 (C), pH 8 (D), pH 9 (E), pH 10 (F), pH 11 (G) and pH 12 (H) at 20 °C for 24 h.

quantitative method (ZAF) with 2–3 iterations. Z-correction considers the average atomic number of the elements forming the matrix material, A-correction takes into account the absorption by the matrix of the emitted X-rays, and F-correction refers to the fluorescent emissions from the matrix. The standards Quartz, Wollastonite, Calcium carbonate and Gold were used. The amount of Si from CO_2H-PMS detected here is in agreement with its content found in the organic matrix from bioceramic in nature, which indicates that morphogenetic aspect of this inorganic material can be well controlled by a very small amount of CO_2H-PMS [1,3,64–68]. Although it is difficult to carry out quantitative determinations by EDS, which is a surface technique, the screening of Si clearly shows no homogeneous distribution as shown as red point at pH 9 and 11 (Fig. 5, insert). This observation provides the

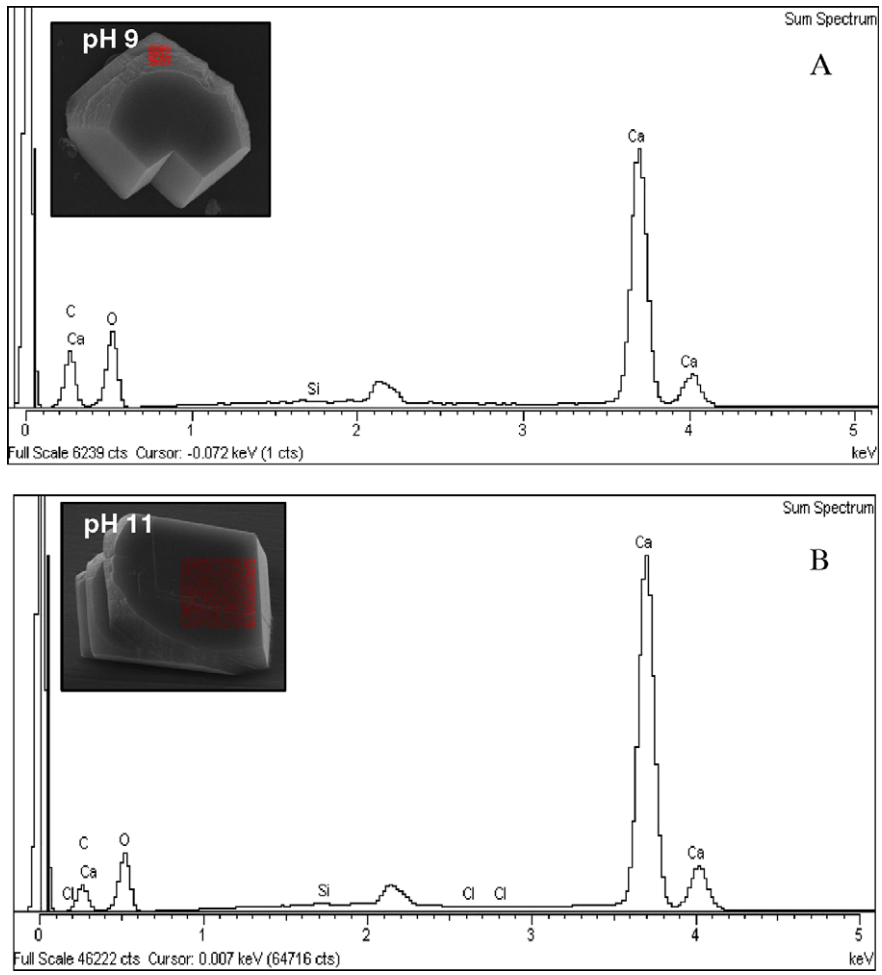

Fig. 5. SEM-EDS of $CaCO_3$ crystals obtained with CO_2H-PMS at pH 9 (A) and pH 11 (B). Red points indicate the distribution of Si atoms onto the surface. (For interpretation of the references to color in this figure legend, the reader is referred to the web version of this article.)

evidence that the Ca^{2+} concentration on the $CaCO_3$ surface is regulated by selective distribution of Si from CO_2H-PMS. We suspect that the variation of the Ca^{2+} content could be regulated by the adsorption of Si from this polymeric template. At different pH, CO_2H-PMS template can undergo changes in carboxylate groups charge adopting different orientations in solution and thereby elicit changes in $CaCO_3$ morphology. We surmise that the crystallization of calcite, which is triggered by the carboxylate groups of CO_2H-PMS, results from a local accumulation of Ca^{2+} ions, which correlates closely with the chemical nature of the polymer and pH of the solution [42]. Finally, EDS revealed the presence of Si from CO_2H-PMS adsorbed onto the modified $CaCO_3$ crystals obtained under all pH values and where Si atoms outside crystals were not found (data not shown) demonstrating the active modifying properties of CO_2H-PMS during the nucleation of $CaCO_3$.

The FTIR spectra of powdered $CaCO_3$ particles formed in the presence of CO_2H-PMS and PDMS-*co*-PHMS at different pH values form pH 7 to 12 through gas diffusion method showed absorptions at 1734 cm^{-1} and at 1022 cm^{-1} attributed to the C=O bond of the carbonyl groups of $CaCO_3$ crystals and to the Si–O–Si indicating the incorporation of this template in the crystal matrix (see Supplementary data). Fig. 6 shows the XRD pattern of the $CaCO_3$ crystals

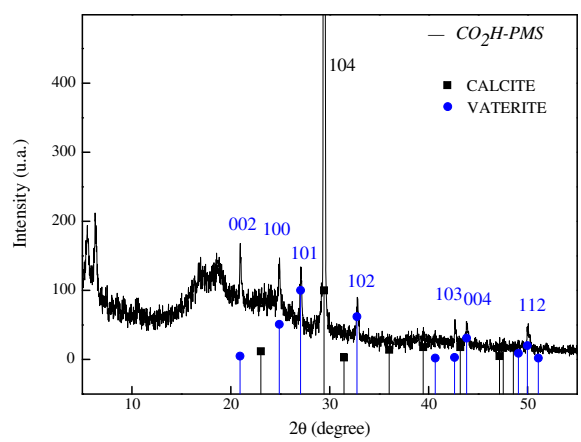

Fig. 6. XRD of $CaCO_3$ crystals obtained in presence of CO_2H-PMS at pH 12.

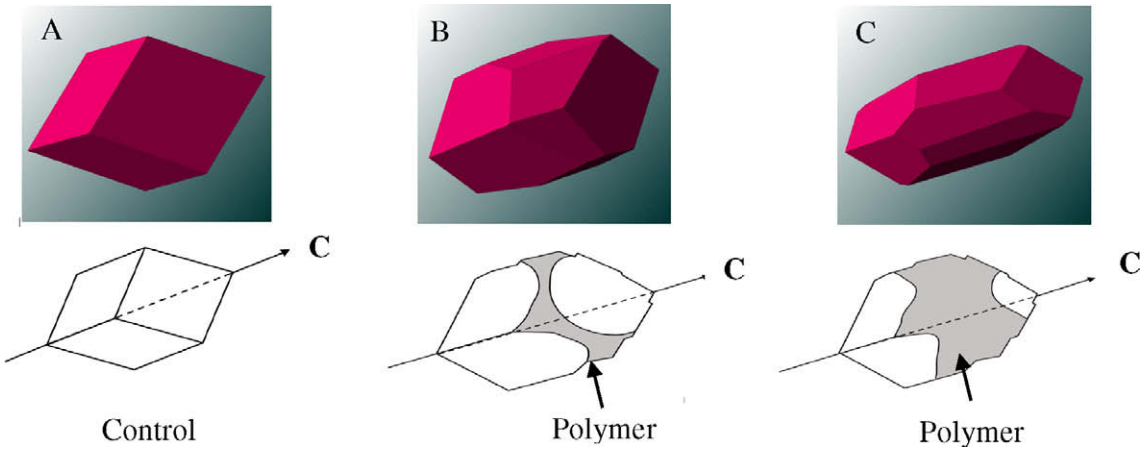

Fig. 7. $CaCO_3$ crystals elongation in the presence of different concentration of CO_2H-PMS at pH 9. Simulation of $CaCO_3$ crystals has been done using Software JCrystal (2008). (A) Control of rhombohedra calcite crystals. (B) Initial modification and (C) fully modification.

grown in the presence of CO_2H-PMS at pH 12. XRD analysis found that calcite and vaterite were the only two principal polymorphs stabilized. It can be seen that the strongest diffraction peak appears at $2\theta = 29.5°$ and is due to the 104 crystallographic face of calcite. However, all the rest of crystalline peaks are ascribed to the diffraction of vaterite, which represents the less thermodynamically stable polymorphs. This result shows the strong modifying capacity of CO_2H-PMS as template during the nucleation step. XRD of $CaCO_3$ grown in the presence of PDMS-*co*-PHMS shows only a crystalline diffraction peak at $2\theta = 29.6°$ confirming the presence of calcite crystals.

A cartoon representation for the elongation of $CaCO_3$ crystals with CO_2H-PMS and simulation of $CaCO_3$ crystal growth using Software JCrystal (2008) are presented in Fig. 7.

The present data strongly suggest the ability of PMS molecules to be used as template for the morphological modification of $CaCO_3$ crystals. This observation allows the understanding of the ability of PMS for changing the

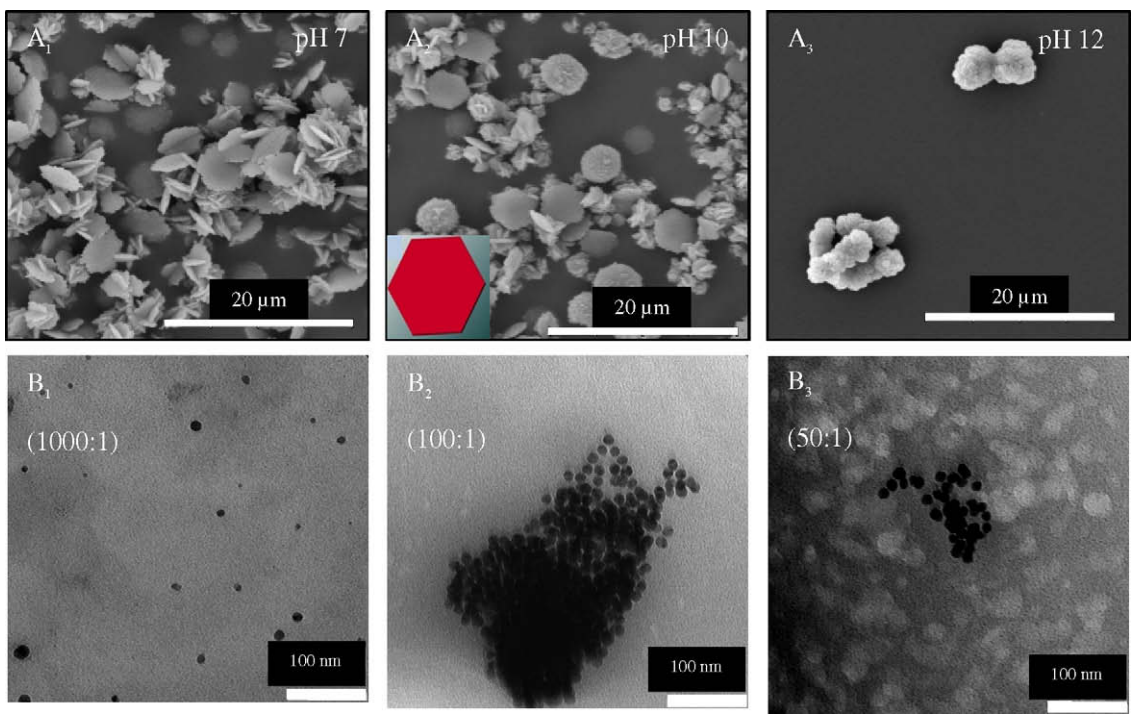

Fig. 8. SEM of $CaCO_3$ with (A) CHI-*g*-CO_2H-PMS and (B) TEM of AuNP coupled with CHI-*g*-CO_2H-PMS at different CHI-*g*-CO_2H-PMS:AuNP ratios. Insert in (A_2) shows the simulation of the observed $CaCO_3$ crystals by using Software JCrystal (2008).

energy landscape during the crystallization process and allows catching a glimpse of interesting future applications in materials. With this in mind the carboxylic groups of CO_2H-PMS was conjugated to primary amine groups of CHI using 1-ethyl-3-(3-dimethylaminopropyl) carbodiimide (EDC) as crosslinker. Thus, different CHIs grafted polysiloxanes (CO_2H-PMS-*g*-CHI) were prepared and then coupled with gold nanoparticles by crosslinking and coupling reactions. These were prepared with different CHI-*g*-CO_2H-PMS:AuNP ratio and their influence on the $CaCO_3$ crystallization was evaluated showing promising results. SEM of $CaCO_3$ obtained in the presence of CO_2H-PMS-*g*-CHI showed that this template is an efficient modulator for stabilizing unstable $CaCO_3$ polymorphs such as vaterite (Fig. 8A_1) or aragonite (Fig. 8A_3) at different pH values. TEM images of AuNP coupled to CO_2H-PMS-*g*-CHI derivatives are shown in Fig. 8B. The determination of AuNP concentrations in CHI-*g*-CO_2H-PMS:AuNP and in the CHI in solution was of 6.26 and 3.77 μg, respectively, performed by instrumental neutron activation analysis (INAA). HRTEM analyses for visualizing the adsorbed AuNP on some specific crystal faces of $CaCO_3$ are under progress.

4. Conclusions

The use of CO_2H-PMS as template can effectively control the morphogenesis and the crystallographic polymorphism of $CaCO_3$ crystals. The composition of the new template and pH of the mineralization solution seem to be crucial during $CaCO_3$ nucleation and growth. Templates based on PMS offer a wide range of possibility for polymer controlled crystallization applications. At different pH values, the carboxylate groups of CO_2H-PMS can undergo different degree of dissociation. Therefore, the polymer adopt different conformation in solution and thereby elicit changes in $CaCO_3$ morphology is obtained. The crystallization of calcite, which is triggered by the carboxylate groups of CO_2H-PMS results from a local accumulation of Ca^{2+} ions, which correlates closely with the pH of the mineralization solution. FTIR analysis is in good agreement with the proposed PMS structures and the resulted $CaCO_3$ particles. SEM analysis showed different $CaCO_3$ crystal morphologies as a function of pH from precursors of $CaCO_3$ nanoparticles to aggregated calcite crystals occurring as short piles (5 μm) at pH 7–9, elongated single crystals (20 μm) at pH 10–11 and donut-like vaterite at pH 12. EDS revealed the presence of Si atoms from CO_2H-PMS adsorbed onto the modified $CaCO_3$ crystals. XRD demonstrated two polymorphs: calcite and vaterite. Unstable $CaCO_3$ polymorphs, i.e., vaterite and aragonite can be stabilized by using CHI-*g*-CO_2H-PMS at different pH. In summary, we demonstrated that the use of PMS and its derivative as templates [58,67,68] provides a viable approach for studying various aspects of biomineralization including production of controlled polymorphs and defined morphologies.

Acknowledgements

This research was supported by FONDECYT 11070136 and FONDAP 11980002 granted by the Chilean Council for Science and Technology (CONICYT). Dr. A. Neira-Carrillo thanks Dr. M. Kogan (University of Chile) for providing the AuNP and to Dr. Habil. Helmut Cölfen and Prof. Markus Antonietti (MPI of Colloids and Interfaces, Golm, Potsdam, Germany) for fruitful discussions. Ingrid Zenke is acknowledged for XRD, Rona Pitschke for SEM and TEM.

Appendix A. Supplementary data

Supplementary data associated with this article can be found, in the online version, at doi:10.1016/j.eurpolymj.2010.03.008.

References

[1] Lowenstam HA, Weiner S. On biomineralization. Oxford: Oxford University Press; 1989. p. 1–50 [chapter 3].
[2] Mann S, Ozin GA. Synthesis of inorganic materials with complex form. Nature 1996;382(6589):313–8.
[3] Meldrum FC. Calcium carbonate in biomineralisation and biomimetic chemistry. Intern Mater Rev 2003;48(3):187–224.
[4] Cölfen H. Precipitation of carbonates: recent progress in controlled production of complex shapes. Curr Opin Colloid Interface Sci 2003;8(1):23–31.
[5] Jones WC. Crystalline properties of spicules of *Leucosolenia complicate*. Q J Microsc Sci 1955;96:129–49.
[6] Aizenberg J, Hanson J, Koetzle TF, Leiserowitz L, Weiner S, Addadi L. Biologically induced reduction in symmetry: a study of crystal texture of calcitic sponge spicules. Chem Eur J 1995;1(7):414–22.
[7] Raup DM. Cristallography of echinoid calcite. J Geol 1959;67:661–74.
[8] Feng QL, Li HB, Zhang DM, Cui FZ, Li HD, Kim TN. Crystallographic alignment of calcite prisms in the oblique prismatic layer of *Mytilus edulis* shell. J Mater Sci 2000;35(13):3337–40.
[9] Addadi L, Weiner S. Control and design principles in biological mineralization. Angew Chem Int Ed 1992;31(2):153–69.
[10] Grassmann O, Lobmann P. Biomimetic nucleation and growth of $CaCO_3$ in hydrogels incorporating carboxylate groups. Biomaterials 2004;25(2):277–82.
[11] Arias JL, Neira-Carrillo A, Arias JI, Escobar C, Bodero M, David M, et al. Sulfated polymers in biological mineralization: a plausible source for bio-inspired engineering. J Mater Chem 2004;14(14):2154–60.
[12] Mann S, Archibald DD, Didymus JM, Douglas T, Heywood BR, Meldrum FC, et al. Crystallization at inorganic–organic interfaces: biominerals and biomimetic synthesis. Science 1993;261(5126):1286–92.
[13] Mann S, Archibald DD, Didymus JM, Heywood BR, Meldrum FC, Wade VJ. Biomineralization: biomimetic potential at the inorganic–organic interface. Mater Res Soc Bull XVII 1992:32–6.
[14] Neira-Carrillo A, Krishna Pai R, Fernández MS, Carreño E, Vasquez Quitral P, Arias JL. Synthesis and characterization of sulfonated polymethylsiloxane polymers as template for crystal growth of $CaCO_3$. Colloid Polym Sci 2009;287:385–93.
[15] Yu SH, Cölfen H. Bio-inspired crystal morphogenesis by hydrophilic polymers. J Mater Chem 2004;14(14):2124–47.
[16] Cölfen H. Double-hydrophilic block copolymers: synthesis and application as novel surfactants and crystal growth modifiers. Macromol Macromol Rapid Commun 2001;22(4):219–52.
[17] Pai RK, Pillai S. Water soluble terpolymer directs the hollow triangular cones of packed calcite needless. Cryst Growth Des 2007;7:215–7.
[18] Tai C, Cheng C. Effect of CO_2 on expansion and saturation of supersaturates solutions. Am Inst Chem Eng J 1998;44(4):1790–9.
[19] Wulff G. Mineral physical reviews. Z Krystallogr 1901;34:449–530.
[20] Didymus JM, Oliver P, Mann S, DeVries AL, Hauschka PV, Westbroek P. Influence of low-molecular-weight and macromolecular organic additives on the morphology of calcium carbonate. J Chem Soc Faraday Trans 1993;89:2891–900.
[21] Weissbuch L, Addadi M, Lahav L, Leiserowitz L. Molecular recognition at crystal interfaces. Science 1991;253(5020):637–45.
[22] Mann S. In: Biomimetic materials science. New York, xii, USA: VCH Publishers; 1996. p. 490.
[23] Marsh ME, Sass RL. Calcium-binding phosphoprotein particles in the extrapallial fluid and innermost shell lamella of clams. J Exp Zool 1983;226(2):193–203.
[24] Politi Y, Arad T, Klein E, Weiner S, Addadi L. Sea urchin spine calcite forms via a transient amorphous calcium carbonate phase. Science 2004;306(5699):1161–4.

[25] Aizenberg J, Ilan S, Weiner S, Addadi L. Intracrystalline macromolecules are involved in the morphogenesis of calcitic sponge spicules. Connect Tissue Res 1996;34(4):255–61.
[26] Aizenberg J, Hanson J, Koetzle TF, Weiner S, Addadi L. Control of macromolecule distribution within synthetic and biogenic single calcite crystals. J Am Chem Soc 1997;119(5):881–6.
[27] Hattan SJ, Laue TM, Chasteen ND. Purification and characterization of a novel calcium-binding protein from the extrapallial fluid of the mollusk *Mytilus eduli*. J Biol Chem 2001;276(6):4461–8.
[28] Wong B, Brisdon J, Heywood B, Hodson A, Mann S. Polymer-mediated crystallisation of inorganic solids: calcite nucleation on the surfaces of inorganic polymers. J Mater Chem 1994;4:1387–92.
[29] Brook MA. Silicon in organic, organometallic, and polymer chemistry. John Wiley & Sons Inc.; 2000.
[30] Abe Y, Gunji T. Oligo- and polysiloxanes. Prog Polym Sci 2004; 29(3):149–82.
[31] Jones RG, Ando W, Chojnowski J. Silicon-containing polymers. Dordrecht: Kluwer Academic Publishers; 2000.
[32] Marciniec B, Gulinski J. Hydrosilylation. In: Maciejewski H, Horvath IT, editors. Encyclopedia of catalysis, vol. 4. New York: Wiley; 2000.
[33] Hu S, Ren X, Bachman M, Sims CE, Li GP, Allbritton NL. Tailoring the surface properties of poly(dimethylsiloxane) microfluidic devices. Langmuir 2004;20:5569–74.
[34] Sia SK, Whitesides GM. Microfluidic devices fabricated in poly(dimethylsiloxane) for biological studies. Electrophoresis 2003;24:3563–76.
[35] Wegner G. Functional polymers. Acta Mater 2000;48(1):253–62.
[36] Liu M, Ragheb A, Zelisko P, Brook M. Preparation and applications of silicone emulsions using biopolymers. In: Elaïssari Abdelhamid, editor. Biomedical applications of polymer colloids. Mercel Dekker Inc.; 2003. p. 747–65.
[37] Kaneko Y, Sato S, Kadokawa J-I, Iyi NJ. Synthesis of organic–inorganic hybrid hydrogels using rodlike polysiloxane having acrylamido groups as a new cross-linking agent. J Mater Chem 2006;16: 1746–50.
[38] Lee S, Vörös J. An aqueous-based surface modification of poly(dimethylsiloxane) with poly(ethylene glycol) to prevent biofouling. Langmuir 2005;21:11957–62.
[39] Zhang XD, Macosko CW, Davis HT, Nikolov AD, Wasan DT. Role of silicone surfactant in flexible polyurethane foam. J Colloid Interface Sci 1999;215:270–9.
[40] Ojima I. The Hydrosilylation Reaction. In: Patai S, Rappoport Z, editors. The Chemistry of Organic Silicon Compounds, vol.1; 1989. p. 1479-99 [chapter 25].
[41] Speier LJ. Homogeneous catalysis of hydrosilation by transition metals: advanced organic chemistry, vol. 17. New York: Academic Press; 1979. p. 673.
[42] Dominguez-Vera JM, Gautron J, Garcia-Ruiz JM, Nys Y. The effect of avian uterine fluid on the growth behaviour of calcite crystals. Poultry Sci 2000;79:901–7.
[43] Neira-Carrillo A. Ph.D. Thesis. Síntesis vía Catiónica de Derivados de Polisiloxanos-Polisilazanos – Precursores de Materiales Cerámicos y de Agentes de Dispersión y Mineralización. University of Concepción; 2003.
[44] Yazdani-Pedram M, Vega H, Quijada R. Melt functionalization of polypropylene with methyl esters of itaconic acid. Polymer 2001;42(10):4751–8.
[45] Neira-Carrillo A, Yazdani-Pedram M, Retuert J, Díaz-Dosque M, Gallois S, Arias JL. Selective crystallization of calcium salts by poly(acrylate)-grafted chitosan. J Colloid Interface Sci 2005;286:134–41.
[46] Apfel MA, Finkelmann H, Janini GM, Laub RJ, Lühmann B-H, Price A, et al. Synthesis and properties of high-temperature mesomorphic polysiloxane (MEPSIL) solvents: biphenyl- and terphenyl-based nematic systems. Anal Chem 1985;57:651–8.
[47] Neira-Carrillo A, Pai RK, Fuenzalida VM, Fernández MS, Retuert J, Arias JL. Calcium carbonate growth modification by constituents released from porous cellulose filter membranes. J Chil Chem Soc 2008;53(2):1469–73.
[48] Arias JI, Jure C, Wiff JP, Fernández MS, Fuenzalida V, Arias JL. Effect of sulfate content of biomacromolecules on the crystallization of calcium carbonate. Mater Res Soc Proc 2002;711:243–8.
[49] Neira-Carrillo A, Fernández MS, Retuert J, Arias JL. Effect of the crystallization chamber design on the occurrence of calcium carbonate polymorphs using the sitting-drop method. Architecture and application of biomaterials and biomolecular materials. In: Barron AE. Klok HA, Deming TJ, editors. Mater Res Soc Proc 2004; EXS-1 H6.18. p. 1–6.
[50] Fernández MS, Passalacqua K, Arias JI, Arias JL. Partial biomimetic reconstruction of avian eggshell formation. J Struct Biol 2004; 148(1):1–10.
[51] Neira-Carrillo A, Retuert J, Martínez F, Arias JL. Effect of crosslinked chitosan as a constrained volume on the in vitro calcium carbonate crystallization. J Chil Chem Soc 2008;53(1):1367–72.
[52] Neira-Carrillo A, Acevedo DF, Peralta DO, Barbero C, Cölfen H, Arias JL. Influence of conducting polymers based on carboxylated polyaniline on *in vitro* $CaCO_3$ crystallization. Langmuir 2008; 24(21):12496–507.
[53] Pouchert JC. The Aldrich library of infrared spectra. 2nd ed. Milwaukee, Wisconsin, USA: Aldrich Chemical Co. Inc.; 1975.
[54] Rodríguez-Baeza M, Neira CA, Aguilera JC. Thermogravimetric studied on the formation of crosslinked structures in the synthesis of poly(methlysiloxane). J Chil Chem Soc 2003;48(2):72–7.
[55] Lopez-Machado MA, Yazdani-Pedram M, Retuert J, Quijada R. Effect of monomethyl itaconate grafted HDPE and EPR on the compatibilidad and properties of HDPE/EPR blends. J Appl Polym Sci 2003;89:2239–48.
[56] Kim IW, DiMasi E, Evans JS. Identification of mineral modulation sequences within the nacre-associated oyster shell protein, n16. Cryst Growth Des 2004;4(6):1113–8.
[57] Kim W, Robertson RE, Zand R. Effects of some nonionic polymeric additives on the crystallization of calcium carbonate. Cryst Growth Des 2005;5(2):513–22.
[58] Grassmann O, Lobmann P. Morphogenetic control of calcite crystal growth in sulfonic acid based hydrogels. Chem A Eur J 2003;9(6):1310–6.
[59] Rieger J, Thieme J, Schmidt C. Study of precipitation reactions by X-ray microscopy: $CaCO_3$ precipitation and the effect of polycarboxylates. Langmuir 2000;16(22):8300–5.
[60] Rieger J, Hädicke E, Rau IU, Boeckh D. A rational approach to the mechanisms of incrustation inhibition by polymeric additives. Tenside Surfactants Deterg 1997;34(6):430–5.
[61] Song RQ, Cölfen H, Xu AW, Hartman J, Antonietti M. Polyelectrolyte-directed nanoparticle aggregation: systematic morphogenesis of calcium carbonate by nonclassical crystallization. ACS Nano 2009;3(7):1965–78.
[62] Hare PE, Abelson PH. Amino acid composition of some calcified proteins. Year Book-Carnegie Inst Washington 1965;65:223–32.
[63] Ares JR, Pascual A, Ferrer IJ, Sanchez C. A methodology to reduce error sources in the determination of thin film chemical composition by EDAX. Thin Solid Films 2004;450(1):207–10.
[64] Brisdon BJ, Heywood BR, Hodson AGW, Mann S, Wong KKW. Polymer-mediated crystallization of inorganic solids: calcite nucleation on poly(organosiloxane) surfaces. Adv Mater 1993;5(1): 49–51.
[65] Wong KKW, Brisdon BJ, Heywood BR, Hodson AGW, Mann S. Polymer-mediated crystallization of inorganic solids: calcite nucleation on the surfaces of inorganic polymers. J Mater Chem 1994;4:1387–92.
[66] Dove PM, DeYoreo JJ, Weiner S. Biomineralization. Rev Mineral Geochem Mineral Soc Am 2003;54:151–87.
[67] Petrova RI, Swift JA. Selective growth and distribution of crystalline enantiomers in hydrogels. J Am Chem Soc 2004;126(4):1168–73.
[68] Li H, Estroff LA. Hydrogels coupled with self-assembled monolayers: an in vitro matrix to study calcite biomineralization. J Am Chem Soc 2007;129(17):5480–3.